AMERICAN JOURNAL OF PHYSIOLOGY
HEART AND CIRCULATORY PHYSIOLOGY

Am J Physiol Heart Circ Physiol 321: H217–H227, 2021.
First published June 18, 2021; doi:10.1152/ajpheart.01002.2020

RESEARCH ARTICLE

Cardiovascular Neurohormonal Regulation

Functional hyperactivity in long QT syndrome type 1 pluripotent stem cell-derived sympathetic neurons

Annika Winbo,[1,2,3,4,5] Suganeya Ramanan,[1,2] Emily Eugster,[6] Annika Rydberg,[5] Stefan Jovinge,[6,7] Jonathan R. Skinner,[2,3,4] and Johanna M. Montgomery[1,2]

[1]*Department of Physiology, University of Auckland, Auckland, New Zealand;* [2]*Manaaki Mānawa Centre for Heart Research, University of Auckland, Auckland, New Zealand;* [3]*Department of Paediatric and Congenital Cardiac Services, Starship Children's Hospital, Auckland, New Zealand;* [4]*The Cardiac Inherited Disease Group (CIDG), Auckland, New Zealand;* [5]*Department of Clinical Sciences, Pediatrics, Umeå University, Umeå, Sweden;* [6]*DeVos Cardiovascular Research Program Spectrum Health/Van Andel Research Institute, Grand Rapids, Michigan; and* [7]*Cardiovascular Institute, Stanford University of Medicine, Stanford, California*

Abstract

Sympathetic activation is an established trigger of life-threatening cardiac events in long QT syndrome type 1 (LQT1). *KCNQ1* loss-of-function variants, which underlie LQT1, have been associated with both cardiac arrhythmia and neuronal hyperactivity pathologies. However, the LQT1 sympathetic neuronal phenotype is unknown. Here, we aimed to study human induced pluripotent stem cell (hiPSC)-derived sympathetic neurons (SNs) to evaluate neuronal functional phenotype in LQT1. We generated hiPSC-SNs from two patients with LQT1 with a history of sympathetically triggered arrhythmia and *KCNQ1* loss-of-function genotypes (c.781_782delinsTC and p.S349W/p.R518X). Characterization of hiPSC-SNs was performed using immunohistochemistry, enzyme-linked immunosorbent assay, and whole cell patch clamp electrophysiology, and functional LQT1 hiPSC-SN phenotypes compared with healthy control (WT) hiPSC-SNs. hiPSC-SNs stained positive for tyrosine hydroxylase, peripherin, KCNQ1, and secreted norepinephrine. hiPSC-SNs at 60 ± 2.2 days in vitro had healthy resting membrane potentials (−60 ± 1.3 mV), and fired rapid action potentials with mature kinetics in response to stimulation. Significant hyperactivity in LQT1 hiPSC-SNs was evident via increased norepinephrine release, increased spontaneous action potential frequency, increased total inward current density, and reduced afterhyperpolarization, compared with age-matched WT hiPSC-SNs. A significantly higher action potential frequency upon current injection and larger synaptic current amplitudes in compound heterozygous p.S349W/p.R518X hiPSC-SNs compared with heterozygous c.781_782delinsTC hiPSC-SNs was also observed, suggesting a potential genotype-phenotype correlation. Together, our data reveal increased neurotransmission and excitability in heterozygous and compound heterozygous patient-derived LQT1 sympathetic neurons, suggesting that the cellular arrhythmogenic potential in LQT1 is not restricted to cardiomyocytes.

NEW & NOTEWORTHY Here, we present the first study of patient-derived LQT1 sympathetic neurons that are norepinephrine secreting, and electrophysiologically functional, in vitro. Our data reveal a novel LQT1 sympathetic neuronal phenotype of increased neurotransmission and excitability. The identified sympathetic neuronal hyperactivity phenotype is of particular relevance as it could contribute to the mechanisms underlying sympathetically triggered arrhythmia in LQT1.

arrhythmia mechanisms; human induced pluripotent stem cells; long QT syndrome; sympathetic hyperactivity; sympathetic neurons

INTRODUCTION

Sympathetic activity modulates ventricular repolarization, and its dysregulation or hyperactivity contributes to the pathophysiology of both primary and secondary cardiovascular disease (1, 2). Increased β-adrenergic signaling during emotional or physical stress is an established trigger of life-threatening cardiac events in the familial long QT syndrome (LQTS), particularly for the most common subtype, LQTS type 1 (LQT1) (2–5). LQT1 is caused by loss-of-function variants in the *KCNQ1* gene, which encodes the alpha-subunit of the tetrameric Kv7.1 voltage-gated potassium channel that is expressed in tissues throughout the human body (7). In the heart, Kv7.1 generates the slow rectifier potassium current (I_{Ks}), which increases in the presence of catecholamines and stabilizes heart rhythm during faster

Correspondence: A. Winbo (a.winbo@auckland.ac.nz).
Submitted 21 December 2020 / Revised 3 June 2021 / Accepted 8 June 2021

beating rates by shortening ventricular repolarization (6–8). In LQT1, the resultant relative cardiac action potential prolongation during sympathetic activation increases the risk for arrhythmogenic early afterdepolarizations via reactivation of L-type calcium channels (9). The major preventive therapeutic options for patients with LQT1 are neuromodulators that target the sympathetic nervous system (β-blockers and cardiac sympathetic denervation); however, the cellular mechanisms underlying sympathetic triggering of LQT1 arrhythmia remains incompletely characterized (2, 5).

Importantly, neuronal *KCNQ1* expression has been verified in human neuronal networks, and *KCNQ1* loss-of-function mutations are associated with human neuronal hyperactivity pathologies, including sudden unexplained death in epilepsy (10). In a clinical study, 22% of patients with LQT1 had a clinical seizure phenotype, together suggesting that central neurons can be affected in patients with LQT1 (10, 11). However, LQT1 sympathetic neuronal phenotype has not been studied in human-derived cells (2, 5).

Patient-derived human induced pluripotent stem cells (hiPSCs) have emerged as a tool to model inherited arrhythmias. Cardiomyocytes differentiated from LQTS hiPSCs emulate the disease phenotype including ventricular action potential prolongation and emergence of arrhythmogenic early afterdepolarizsations in LQT1 hiPSC-cardiomyocytes in response to sympathomimetics (12–14). Human stem cells can also be differentiated into sympathetic-like neurons (15, 16), and recently we developed norepinephrine-secreting sympathetic neurons and functional neuronal-cardiomyocyte cocultures from hiPSCs (17).

Here, we describe the functional and electrophysiological characterization of LQT1 hiPSC-sympathetic neurons (SNs) from two patients with LQT1 with a history of sympathetically triggered events and heterozygous or compound heterozygous *KCNQ1* loss-of-function genotype.

METHODS

Participants with LQT1 and Clinical History

The study has been approved by Institutional Review Boards in Auckland, New Zealand (Health and Disability Ethics Committees: 17/NTA/226), and in Umeå, Sweden (Regional Ethical Review Board in Umeå: Dnr 05-127 M), and all participants have provided written informed consent.

The first patient with LQT1 is a young adult female with a novel *KCNQ1* loss-of-function variant (c.781_782delinsTC, Fig. 1, *A* and *B*) (18). She presented with syncope after running up a flight of stairs at age 15. The QTc of the patient is 530 ms [measured on a 12-lead electrocardiogram (ECG) by an experienced clinician in lead II and corrected for heart rate using Bazett's formula], and her two affected sisters both have a QTc $>$ 500 ms (588 ms and 521 ms, respectively) (18). The patient's family history includes four sudden deaths, three below 40 yr of age and one occurring in a 10-yr-old child during a running race. The patient is treated with β-blockers and has undergone left cardiac sympathetic denervation. The second patient with LQT1 is a young adult male with a severe compound heterozygous genotype consisting of two distinct *KCNQ1* loss-of-function variants, one inherited from each parent (p.S349W/p.R518X, c.1046C>G/c.1552C>T, Fig. 1, *C–E*) (19). The patient's clinical cardiac phenotype includes a prolonged QT interval (QTc 557 ms, measured on a 12-lead ECG by an experienced clinician in lead II and corrected for heart rate using Bazett's formula), an early debut of cardiac symptoms (intrauterine bradycardia and first syncope at 14 mo of age), and multiple sympathetically triggered cardiac events, including aborted cardiac arrests (19, 20). Described triggers include physical activity/sports, fear/anger, swimming, and falling into water/water immersion (19). The patient is treated with β-blockers, left cardiac sympathetic denervation, has an implantable cardioverter defibrillator (ICD), and has received appropriate ICD therapy on multiple occasions (example of appropriate shock terminating ventricular fibrillation as presented in Fig. 1*E*). In addition to his cardiac phenotype, the patient's *KCNQ1* function loss-related extracardiac phenotype includes partial (incomplete) sensorineural deafness, mild vestibular dysfunction, and symptoms/signs related to gastrointestinal dysfunction (19, 21, 22).

Tissue Culture Methods

Peripheral blood mononuclear cells from both patients were reprogrammed using an integration-free kit (CytoTune-iPS 2.0 Sendai Reprogramming Kit, Invitrogen, Life Technologies, now Thermo Fisher, Cat. Nos. A16517 and A16518). Putative hiPSC clones were validated by immunostaining for pluripotency markers SSEA4, Oct4, Tra-1-60, and Sox2.

Generation of hiPSC-SNs was performed using our published methods (17). The functional phenotypes of patient-derived hiPSC-SNs were compared across LQT1 genotypes and to the functional phenotypes of hiPSC-SNs derived from healthy control hiPSCs (wildtype, WT), and generated at the same time as the LQT1 hiPSC-SNs (17). Our detailed tissue culture protocols are available at https://figshare.com/articles/online_resource/Functional_Coculture_of_Sympathetic_Neurons_and_Cardiomyocytes_Derived_from_Human_Induced_Pluripotent_Stem_Cells/12756239. In brief, sympathetic neurons were generated from LQT1 and WT hiPSCs using our optimized neuronal induction and differentiation protocol, based on previously published protocols (15, 23), and modified for feeder-free culture conditions (17). For LQT1 and WT genotypes, neuronal differentiation was repeated to ensure phenotypic consistency over multiple differentiation rounds (two times for c.781_782delinsTC, and $\geq$5 times for p.S349W/p.R518X and WT, respectively). Characterization of cellular phenotype, using immunohistochemistry staining, enzyme-linked immunosorbent assay, and electrophysiological whole cell patch clamp experiments, was performed in hiPSC-SNs matured to $\geq$48 days since pluripotency, based on our previous data on age-dependent maturity in hiPSC-SNs (17).

Immunohistochemistry and Imaging

For immunohistochemistry, cells were fixed in 4% paraformaldehyde for 20 min at room temperature, permeabilized in 0.1% TritonX-100/PBS, and labeled with primary antibodies for tyrosine hydroxylase (1/500, guinea pig polyclonal anti-serum 2, Cat. No. 213 104, Synaptic Systems),

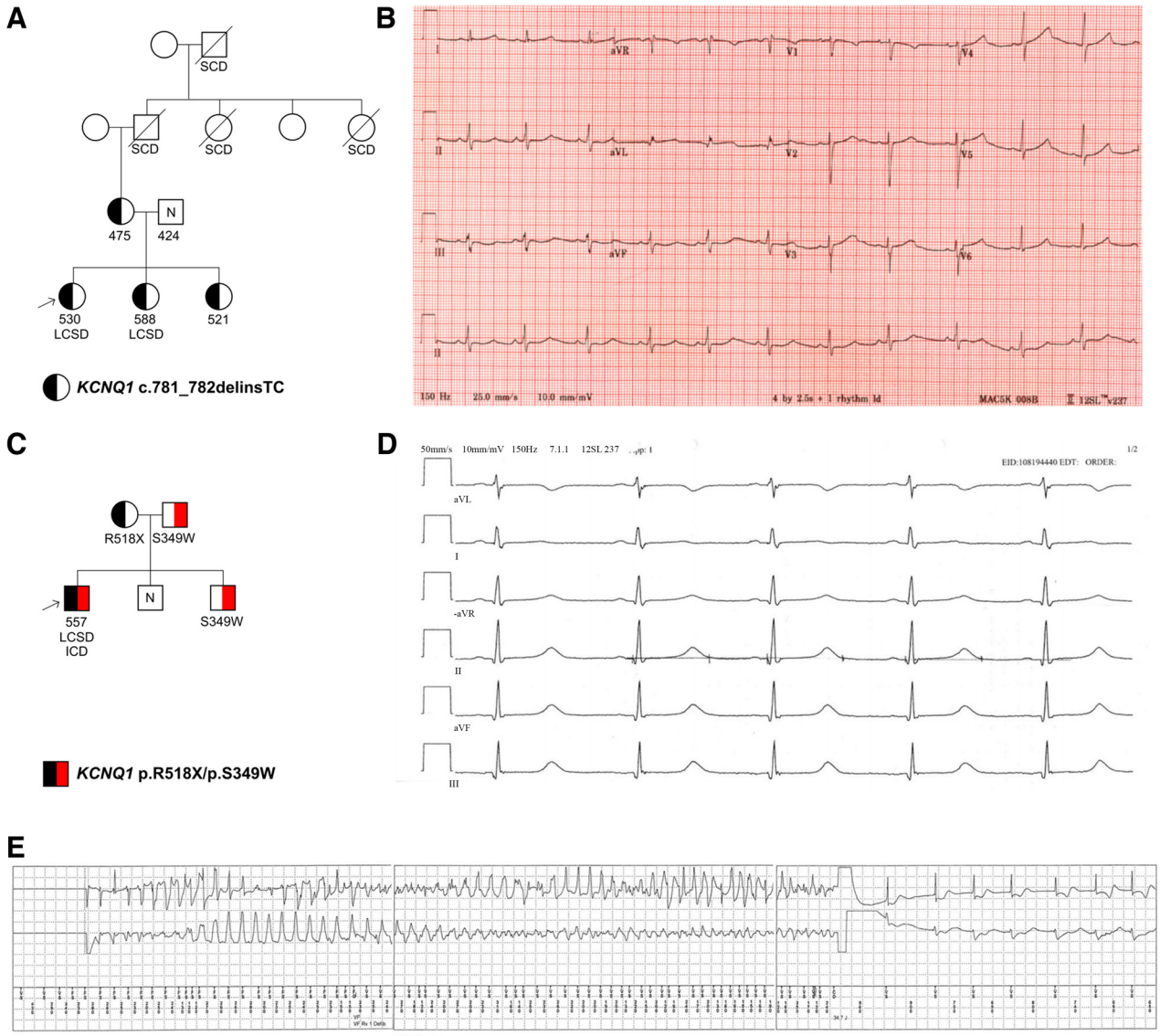

Figure 1. Pedigrees depicting familial long QT syndrome type 1 (LQT1) genotypes and clinical data for included probands (arrows). *A*: family with a history of multiple sudden cardiac deaths segregating the c.781_782insdelTC splice variant in *KCNQ1*. The proband is a carrier of the familial variant (heterozygous genotype). *B*: 12-lead resting electrocardiogram for the c.781_782insdelTC proband, recorded at 25 mm/s, 10 mm/mV. *C*: family segregating two *KCNQ1* variants, p.R518X (c.1552C>T, truncating mutation) and p.S349W (c.1046C>G, missense mutation). The proband carries both variants (compound heterozygous genotype). *D*: 12-lead resting electrocardiogram for the p.S349W/p.R518X proband, recorded at 50 mm/s, 10 mm/mV, showing limb leads. *E*: rhythm strip for the p.S349W/p.R518X proband, recorded at 25 mm/s, showing spontaneous ventricular fibrillation (interval <290 ms, rate >207 beats/min) triggered while playing land hockey, and successful termination of the arrhythmia by a 34.7 J implantable cardioverter defibrillator (ICD) shock. QTc in ms is given directly below symbols (square: male, circle: female). N-genotype negative (−/−); half-filled symbol: heterozygous LQT1 genotype (+/−); double filled symbol: compound heterozygous LQT1 genotype (+/+). LCSD, left cardiac sympathetic denervation; SCD, sudden cardiac death.

peripherin (1/100, rabbit polyclonal, ab1530, Chemicon), and KCNQ1 (1/50, rabbit polyclonal, APC-022, Alomone laboratories), at 4°C for 20–25 h. After PBS washes, secondary antibodies (Alexa Fluor 488, 568 and 647, Thermo Fisher; 1:500) and Hoechst nuclear stain solution (Sigma-Aldrich) were applied at room temperature for 1 h and 20 min, respectively. To validate antibodies for specificity, negative controls with no antibodies, primary antibodies only, and secondary antibodies only, were included. Cells were mounted in Citifluor on glass slides, and epifluorescence imaging was performed at ×40 magnification using a ZEISS AXIOPLAN2 Fluorescence Microscope with a Photometrics camera and MetaMorphs version 7.8.3 for acquisition, image processing, and analysis (Molecular devices). Exposure times were optimized per antibody and were kept consistent across all image acquisitions. Images were generated in ImageJ.

Measurement of Norepinephrine Concentrations

An enzyme-linked immunosorbent assay was used to measure norepinephrine concentration in the culture medium according to the manufacturer's instruction [Aviva Systems Biology Norepinephrine ELISA Kit (OKEH02565)].

Norepinephrine concentration was measured in fresh medium after a 15-min incubation time, either in HBSS or HBSS with 1 μM tetrodotoxin (TTX). Norepinephrine release in LQT1 hiPSC-SN cultures was quantified in pg/mL and presented as means ± SE and fold change (norepinephrine release normalized to the mean norepinephrine release measured in WT hiPSC-SN cultures of the same day in vitro, plated at the same density, and analyzed concurrently with each assay using its own optical density standards).

Whole Cell Electrophysiology Recordings

Whole cell patch clamp recordings were performed at room temperature in hiPSC-SN monocultures, grown on 12-mm Geltrex covered glass coverslips, perfused with extracellular solution containing (in mM) 119 NaCl, 2.5 KCl, 2.5 $CaCl_2$, 1 Na_2HPO_4, 1.3 $MgSO_4$, 26.2 $NaHCO_3$, 11 D-(+)-glucose, adjusted to pH 7.4 with NaOH (17). The internal solution consisted of (in mM): 120 K gluconate, 40 HEPES, 5 $MgCl_2$, 2 Na-ATP, 0.3 Na-GTP, pH adjusted to 7.2 with KOH (34). Recordings were acquired with a MultiClamp 700B amplifier, low-pass filtered at 10 kHz, without leak subtraction, and analyzed using pCLAMP 10.2 software (17). Recordings with an access resistance exceeding 20 MΩ were discarded (17).

To characterize active and passive membrane properties, the resting membrane potential (mV), cell capacitance (pF), and membrane resistance (MΩ) for each hiPSC-SN were recorded (17). Spontaneous hiPSC-SN action potential frequency was assessed via 5-min gap-free recordings (17). The hiPSC-derived neurons' propensity to fire action potentials upon current injection was characterized by 100 pA incremental current steps from 100 to 800 pA, with duration of 200 ms per step (17). The proportion of hiPSC-SNs with a phasic versus tonic action potential firing pattern was quantified for each genotype (17). Action potential firing frequency was calculated excluding phasic hiPSC-SNs and compared across genotypes. Action potential characteristics (action potential amplitude, in mV ± SE, upstroke velocity, in mV/ms ± SE, and action potential duration at 50% repolarization, in ms ± SE) were measured in the first elicited action potential induced by current injection (100 pA to 300 pA), including both phasic and tonic hiPSC-SNs (17).

Total current-voltage (*I-V* or pA/mV) relations were determined using a voltage step protocol. hiPSC-SNs were held at −70 mV before stepping to between −80 mV and +70 mV for 1 s, with 10 mV increment per voltage step. To obtain total peak current density voltage curves [(pA/pF)/mV], total peak current measurements (pA) were presented normalized to the cell membrane capacitance (pF) (17). To capture spontaneous hiPSC-SN synaptic current activity, cells were voltage clamped close to resting membrane potential (−70 mV) and 5-min gap-free recordings performed (17). For each cell, 50 consecutive synaptic currents were manually detected while blinded to genotype, and the amplitudes measured using MiniAnalysis (Synaptosoft Version 6.0.7). Action currents, identified by their larger (>1 mA) amplitudes and faster decay kinetics, were not included in the analysis. The collated synaptic current data were presented using cumulative probability plots and column graphs representing mean pA ± standard error means. For visual comparison, synaptic current amplitude histograms were constructed with bin width 2 pA, except for synaptic current amplitudes ≥100 pA that were binned together (17).

Statistical Analysis

For continuous variables, statistical comparison between the three separate genotype groups (c.781_782delinsTC, p.S349W/p.R518X, and WT) was done using analysis of variance (ANOVA), followed by post hoc comparison between groups when appropriate (Tukey's multiple comparisons test). For independent comparison between two separate groups, Student's *t* test was used for continuous variables and χ^2 test was used for dichotomous variables/proportions. A two-tailed value of $P < 0.05$ was considered statistically significant. Continuous variables are presented as means ± SE, and dichotomous variables as *n* (percent). GraphPad Prism 8.4.3 for Windows (GraphPad Software, San Diego, CA, www.graphpad.com) was used for analyses and graphs. Inkscape Project, 2020 (available at: https://inkscape.org) was used to generate composite images.

RESULTS

Immunohistochemical Characterization

To verify the sympathetic phenotype, LQT1 and WT hiPSC-SNs were immunostained for tyrosine hydroxylase (TH), the rate-limiting enzyme needed for norepinephrine synthesis, peripherin, an intermediate filament expressed in neurons of the peripheral nervous system, and KCNQ1, specifically an extracellular epitope of the *KCNQ1*-encoded Kv7.1 potassium channel. Both WT and LQT1 hiPSC-SNs expressed all three markers, as evident by diffuse TH, peripherin (PRPH), and KCNQ1 expression in the soma and dendrites (Fig. 2, *A–L*).

Enzyme-Linked Immunosorbent Assay of Norepinephrine Release

To quantify presynaptic release of norepinephrine from hiPSC-SNs, we measured the concentration of norepinephrine in the culture medium of LQT1 neuronal cultures, using an enzyme-linked immunosorbent assay (Fig. 3). Norepinephrine release was significantly increased in LQT1 hiPSC-SN cultures, $P = 0.041$ across the three genotype groups by one-way ANOVA, Fig. 3*A*. On average, a fourfold increase in norepinephrine release (fold change 4.1 ± 1.2) was detected in culture medium from LQT1 hiPSC-SNs compared with matched WT cultures [mean norepinephrine concentration 62 ± 23 pg/mL in LQT1 hiPSC-SN cultures ($n = 12$) vs. 14 ± 5 pg/mL in WT hiPSC-SN cultures ($n = 8$), across all assays]. The respective fold change for each LQT1 genotype was 3.3 ± 1.1 for c.781_782delinsTC ($n = 8$) and 6.2 ± 2.8 for p.S349W/p.R518X ($n = 4$), $P = 0.290$ between LQT1 genotypes using Tukey's multiple comparisons test.

To probe further into the mechanisms of norepinephrine release in LQT1 hiPSC-SNs, norepinephrine concentrations were measured in culture medium at baseline and following sodium channel block by 1 μM TTX. Among LQT1 +/− cultures with a baseline norepinephrine concentration of 38 ± 5.8 pg/mL, $n = 6$, norepinephrine release was either reduced (in 1/6; from 42 to 20 pg/mL) or abolished (in 5/6) after exposure to TTX (Fig. 3*B*).

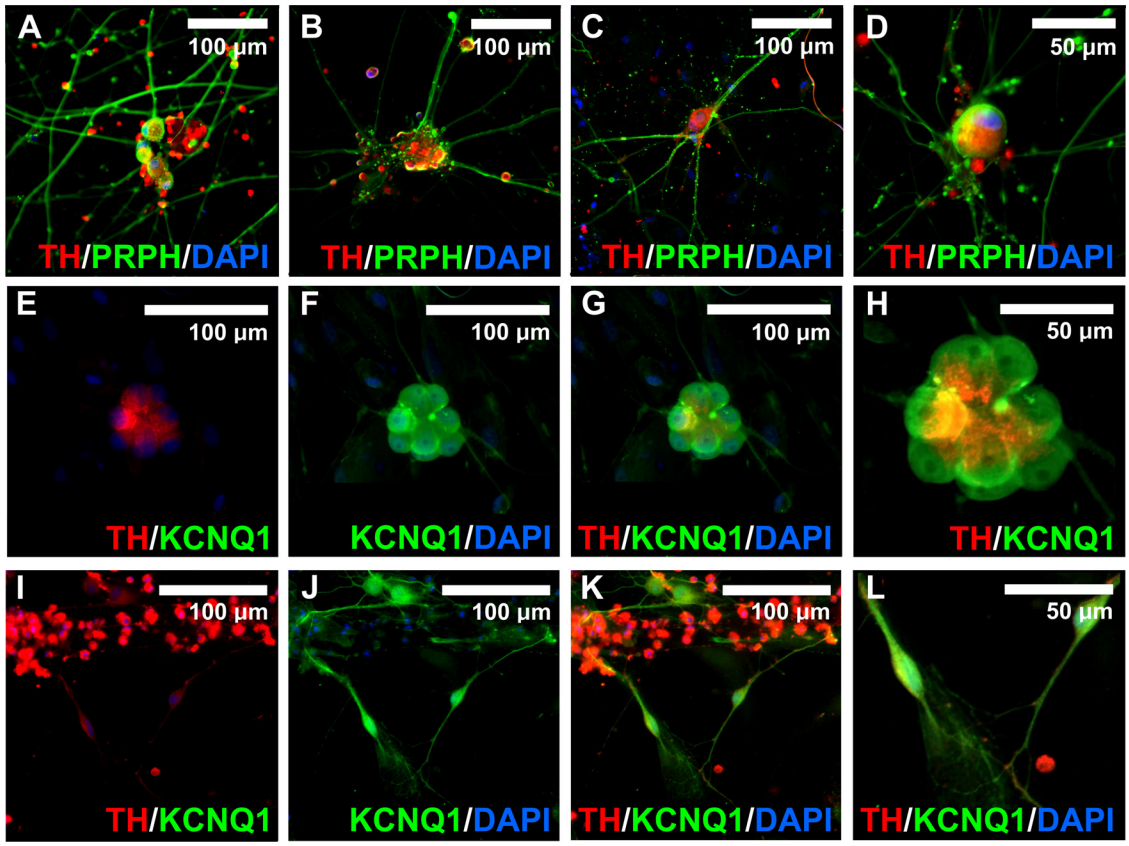

Figure 2. Immunohistochemical staining supporting a sympathetic neuronal fate and *KCNQ1* expression in human induced pluripotent stem cell (hiPSC)-derived cells. *A–D*: long QT syndrome type 1 (LQT1) and wild-type (WT) hiPSC-sympathetic neurons (SNs) stained positive for sympathetic marker TH (red), peripheral neuronal marker peripherin (PRPH), and nuclear marker DAPI (blue). *A*: WT hiPSC-SNs. *B*: heterozygous LQT1 hiPSC-SNs (c.781_782delinsTC). *C*: compound heterozygous LQT1 hiPSC-SN (p.S349W/p.R518X). *D*: WT hiPSC-SN. *E–H*: WT hiPSC-SNs stained positive for TH (red), nuclear marker DAPI (blue), and KCNQ1 extracellular potassium channel marker (green). *I–L*: LQT1 (p.S349W/p.R518X) hiPSC-SNs stained positive for TH (red), DAPI (blue), and KCNQ1 (green). All characterization (*A–L*) was performed in hiPSC-SNs ≥48 days in vitro (24).

Whole Cell Patch-Clamp Electrophysiology Characterization

As sympathetic neurons are excitable cells, we used whole cell electrophysiology recordings to characterize neuronal functional phenotype. During baseline recordings in current clamp, 73% of LQT1 hiPSC-SNs (35/48) were more likely to fire action potentials spontaneously (75% or 12/16 for p.R518X/p.S349W; 72% or 23/32 for c.781_782delinsTC), compared with WT (40% or 12/30; P = 0.004 between LQT1 and WT, χ^2 test). A summary of hiPSC-SN characteristics, stratified by genotype and action potential firing pattern, is presented in Table 1. Days in vitro, resting membrane potential, membrane capacitance, and membrane resistance was comparable between LQT1 (n = 35) and WT (n = 22) hiPSC-SNs, Table 1. However, LQT1 hiPSC-SNs were more likely to have a tonic (multiple action potential) firing pattern (100% or 35/35, p.S349W/p.R518X, n = 16 and 781_782delinsTC, n = 19), compared with WT (73% or 16/22), and to fire at the lowest threshold of current injection, 100 pA, compared with WT (97% vs. 36%, $P < 0.00001$, χ^2 test, Table 1). When comparing the action potential firing frequency of LQT1 and WT hiPSC-SNs with a tonic firing pattern, LQT1 hiPSC-SNs (n = 35) presented with an increased action potential firing frequency across a current injection range of 100–800 pA compared with WT (p.S349W/p.R518X, n = 16, c.781_782delinsT, n = 19, and WT, n = 16 WT, $P < 0.0001$ across all three groups, two-way ANOVA, Fig. 4*A*). Post hoc multiple comparison between groups, with adjusted P values, showed increased action potential firing frequency in compound heterozygous LQT1 hiPSC-SNs (+/+) compared with WT (−/−, P = 0.0008 to $P < 0.0001$), compound heterozygous LQT1 hiPSC-SNs (+/+) compared with heterozygous LQT1 hiPSC-SNs (+/−, $P < 0.05$ to $p < 0.01$), and increased action potential firing frequency in heterozygous LQT1 hiPSC-SNs (+/−) compared with WT (−/−, $P < 0.05$ to $P < 0.01$), Fig. 4*A*).

Afterhyperpolarization (AHP) amplitude was assessed in spontaneously firing hiPSC-SNs, 14 of each genotype. The mean amplitude of the AHP was −4.8 ± 1.2 mV in c.781_782delinsTC, −7.9 ± 1.2 mV in p.S349W/p.R518X, and −8.0 ± 1.3 mV in WT hiPSC-SNs. Example AHP amplitudes from each genotype are presented in Fig. 4, *B–D*. Notably, the AHP was absent in 57% (16/28) of LQT1 hiPSC-SNs, compared with 7% (1/14) in WT hiPSC-SNs, with a significant difference in the proportion of hiPSC-SNs with an AHP between LQT1 genotypes and WT ($P < 0.05$, χ^2 test). The 57% of LQT1 hiPSC-SNs without AHPs constituted 14% presenting with action potentials not followed by an AHP only, and 43% presenting in combination with subsequent afterdepolarizations or excitatory

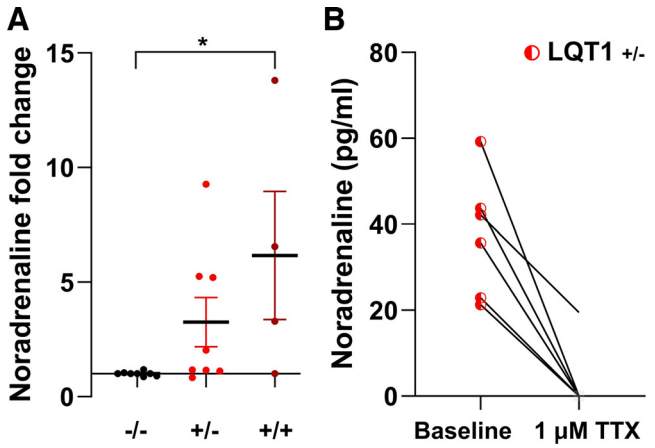

Figure 3. Norepinephrine release in long QT syndrome type 1 (LQT1) human induced pluripotent stem cell (hiPSC)-derived sympathetic neurons (hiPSC-SN) cultures. *A*: norepinephrine release was significantly increased in culture medium from LQT1 hiPSC-SNs compared with matched wild-type (WT) (−/−) cultures, mean fold change 4.1 ± 1.2 for LQT1 (n = 12), 3.3 ± 1.1 for LQT1 (+/−) c.781_782delinsTC (n = 8), and 6.2 ± 2.8 for LQT1 (+/+) p.S349W/p.R518X (n = 4), P = 0.041 across the three genotypes by one-way ANOVA. *B*: following sodium channel block with 1 µM tetrodotoxin (TTX) norepinephrine release was largely abolished in LQT1 (+/−) hiPSC-SN cultures (n = 6). *$P < 0.05$.

postsynaptic potentials, with or without triggered action potentials (Fig. 4, *C* and *D*).

To assess global conductance across ion channels in the hiPSC-SNs, cells were initially held at −70 mV and then a voltage step protocol performed from −80 mV to +70 mV (Fig. 5*A*). Total current density *I-V* curves, i.e., total current corrected for cell capacitance, (pA/pF over mV), were constructed, and showed a significant genotype-dependent difference in total current density (c. 781_782delinsTC, n = 26; p.S349W/p.R518X, n = 25; WT, n = 23, $P < 0.0001$ between the three groups by two-way ANOVA, Fig. 5*A*). Specifically, LQT1 hiPSC-SNs presented with a significantly larger total inward current with its maximum density between +10 mV and +30 mV as compared with WT (adjusted $P < 0.05$ to $P < 0.01$ by Tukey's multiple comparisons test, Fig. 5*A*).

To assess the synaptic input to hiPSC-SNs from other hiPSC-SNs in vitro, neurons were held at −70 mV and the amplitude of 50 consecutive synaptic currents were measured per cell. Synaptic current amplitudes were significantly larger in LQT1 hiPSC-SNs compared with WT (c. 781_782delinsTC, n = 12; p.S349W/p.R518X, n = 12; n = 12 WT, $P < 0.0001$, one-way ANOVA across the three groups, Fig. 5, *B–F*), as evidenced by a right shift in the cumulative probability plots, and amplitude frequency histograms (Fig. 5, *B*, *D–F*). Ad hoc subgroup analysis using Tukey's multiple comparisons test showed synaptic current amplitudes were significantly larger in compound heterozygous LQT1 hiPSC-SNs (p.S349W/p.R518X) as compared with heterozygous LQT1 hiPSC-SNs (c. 781_782delinsTC), P = 0.003, Fig. 5, *B*, *C*, and *F*).

DISCUSSION

Here, we present the first study of human-derived LQT1 sympathetic neurons that are norepinephrine-secreting, and electrophysiologically functional, in vitro. Our data reveal a novel LQT1 sympathetic neuronal phenotype of increased neurotransmission and excitability.

KCNQ1 expression has been reported in multiple regions of the human brain including the brainstem with RT-PCR and channel protein localization (10). In our study, hiPSC-SNs from both WT and patients with LQT1 stained positive for Kv7.1. The effect of dominant *KCNQ1* mutations identified in patients with LQT1 on neuronal activity and arrhythmia propensity has been studied in freely moving mice using simultaneous electroencephalogram (EEG) and ECG recordings, which revealed epileptiform EEG spike discharges and ECG arrhythmias in all heterozygous and homozygous LQT1 mutant mice, whereas WT littermates exhibited no EEG or ECG changes of pathological significance (10). Moreover, in the LQT1 mice, 62% of ECG abnormalities were concurrent with EEG epileptiform discharges (10). There is significant evidence of coincidence between epileptic activity and cardiac arrhythmias in human patients undergoing simultaneous EEG and ECG recordings (25–27). Among patients with LQT1 with confirmed *KCNQ1* loss-of-function mutations, an epileptic phenotype was present in 22% (11). Taken together, these data strongly support that LQT1 mutations could underlie a neuronal hyperexitability phenotype,

Table 1. *Electrophysiological characteristics of WT and LQT1 hiPSC-derived sympathetic neurons in response to current injection*

	WT	WT		LQT1	LQT1		
	WT	Tonic	Phasic	LQT1	(+/−)	(+/+)	*P* Values*
n	**22**	16	6	**35**	19	16	–
Mean age, days after hiPSC stage	60 ± **2.2**	61 ± 2.4	59 ± 5.1	62 ± **1.2**	58 ± 0.8	66 ± 1.9	**0.545**
Resting membrane potential, mV	−60 ± **2.0**	−59 ± 1.4	−61 ± 3.8	−58 ± **0.8**	−56 ± 0.8	−60 ± 1.3	**0.147**
Cell capacitance, pF	81 ± **3.4**	77 ± 3.9	88 ± 6.2	70 ± **4.0**	77 ± 5.7	63 ± 5.2	**0.097**
Membrane resistance, MΩ	122 ± 33	146 ± 42	49 ± 12	138 ± 18	122 ± 22	157 ± 30	**0.645**
Upstroke velocity, mV/ms	181 ± 18	169 ± 20	219 ± 41	202 ± 11	203 ± 14	202 ± 19	**0.301**
Action potential duration at 50%, ms	**2.5** ± **0.2**	2.5 ± 0.2	2.5 ± 0.4	**2.2** ± **0.1**	2.7 ± 0.2	1.7 ± 0.1	**0.220**
Tonic (multiple) firing pattern	**16 (73)**	–	–	**35 (100)**	19 (100)	16 (100)	–
Firing at 100 pA current injection, *n* (%)	**8 (36)**	8 (50)	0	**34 (97)**	19 (100)	15 (94)	**<0.00001**
First firing at 200 pA, *n* (%)	**10 (45)**	8 (50)	2 (33)	**1 (3)**	0	1 (6)	–
First firing at 300 pA, *n* (%)	**4 (18)**	0	4 (67)	**0**	0	0	–

Values are means ± SE or *n* (%). hiPSC, human induced pluripotent stem cell; LQT1, long QT syndrome type 1; LQT1 (+/−), c.718_782delinsTC; LQT1 (+/+)- p.S349W/p.R518X; WT, wild type. *Between all WT (bold) and all LQT1 (bold), as calculated by two-tailed *t* test (continuous variables) or χ^2 test (categorical variables), (−) no testing performed.

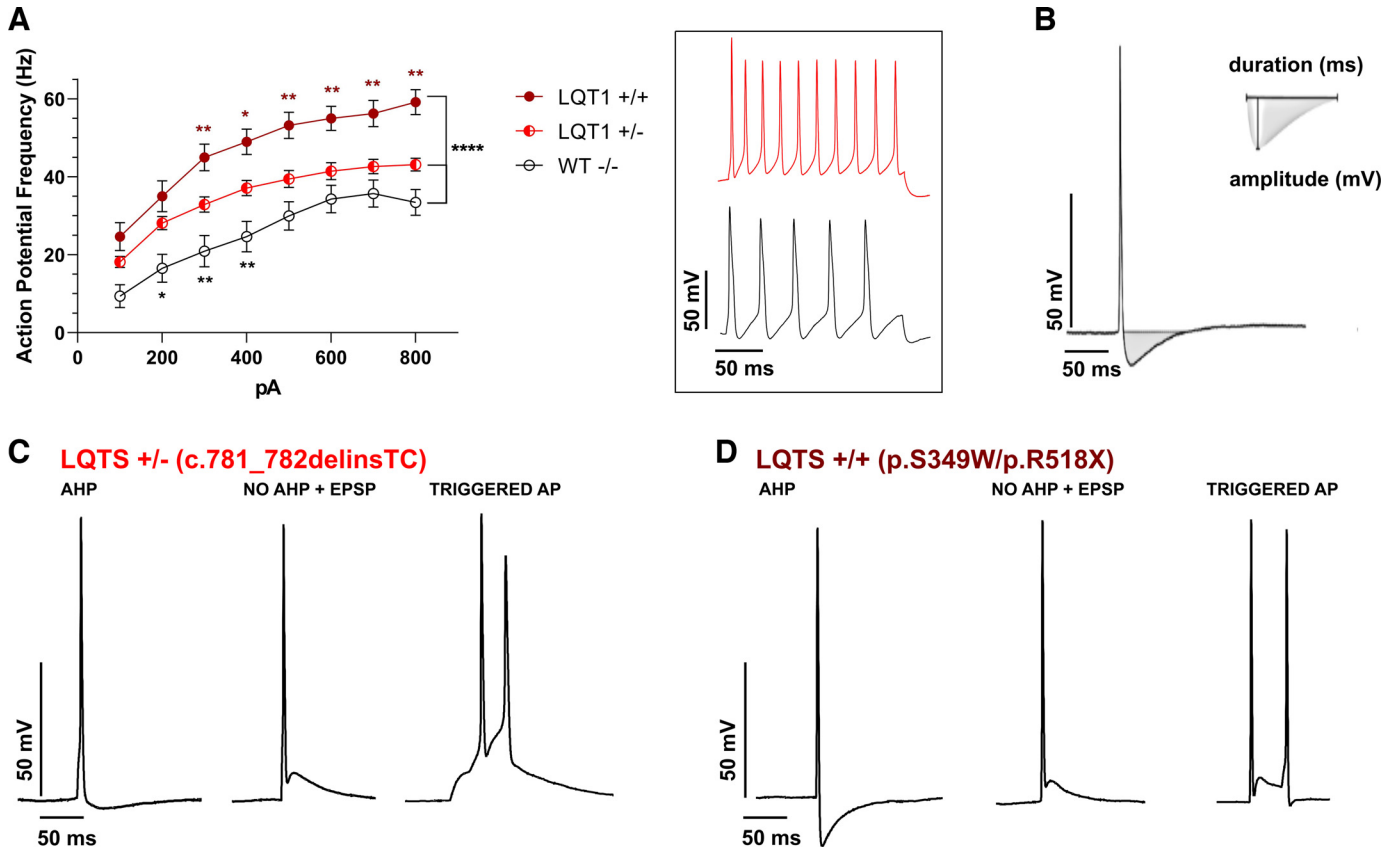

Figure 4. Increased action potential firing frequency and reduced afterhyperpolarization amplitude in long QT syndrome type 1 (LQT1) human induced pluripotent stem cell (hiPSC)-derived sympathetic neurons of heterozygous (+/−) and compound heterozygous (+/+) *KCNQ1* genotype, compared with wild-type (WT) (−/−). *A*: in response to current injection (100–800 pA), action potential firing frequency was significantly increased in LQT1 hiPSC-sympathetic neurons (hiPSC-SNs) compared with WT ($P < 0.0001$, $n = 19$ c.781_782delinsTC; $n = 16$ S394W/R518X; $n = 16$ WT, analyzed by two-way ANOVA across the three groups). Ad hoc subgroup analysis using Tukey's multiple comparisons test further showed action potential firing frequency was significantly increased in LQT1 (+/+) hiPSC-SNs compared with LQT1 (+/−) hiPSC-SNs, adjusted $P < 0.05$ to $P < 0.01$ (red asterisks), and in LQT1 (+/−) hiPSC-SNs compared with WT hiPSC-SNs (−/−), adjusted $P < 0.05$ to $P < 0.01$ (black asterisks). *Inset*: example action potentials from LQT1 (red) and WT (black) hiPSC-SNs. *B–D*: lack of afterhyperpolarization (AHP) following a spontaneous action potential occurred in 57% (16/28) of LQT1 hiPSC-SNs (9/14 c.781_782delinsTC; 7/14 p.S349W/p.R518X9), compared with 7% (1/14) in WT hiPSC-SNs, $P < 0.05$. *B*: representative AHP example from a WT hiPSC-SN (seen in 13/14 cells). *C*: example of AHP (*left*, seen in 5/14 cells) and repolarization/afterdepolarization abnormalities (*middle* and *right*, seen in 9/14 cells) in LQT1 +/− (c.781_782delinsTC) hiPSC-SNs ($n = 14$). *D*: example of AHP (*left*, seen in 7/14 cells) and repolarization/afterdepolarization abnormalities (*middle* and *right*, seen in 7/14 cells) in LQT1 +/+ (p.S349W/p.R518X) hiPSC-SNs ($n = 14$). All characterization (*A–D*) was performed in hiPSC-SNs ≥48 days in vitro (24). AP, action potential; EPSP, excitatory postsynaptic potential. *$P < 0.05$, **$P < 0.01$, and ****$P < 0.0001$.

and support an association between *KCNQ1* function loss, neuronal hyperactivity, and cardiac arrhythmia in LQT1 (10, 11).

The present study includes two *KCNQ1* loss of-of-function genotypes. The novel heterozygous c.781_782delinsTC loss-of-function variant affects the splicing of the *KCNQ1* gene transcript of the allele on which it resides, leading to skipping of exon 6, which encodes S5 and part of the pore domain of the KCNQ1 protein (18). This predicts c.781_782delinsTC to be an unequivocally pathogenic LQT1 variant, however, it is not predicted to affect the function of the wild-type allele, and the functional effect of the heterozygous c.781_782delinsTC genotype in a cellular model is yet to be determined (18). The compound heterozygous p.S349W/p.R518X genotype consists of two mutations, one on each allele. The p.S349W (S6) variant is a missense mutation with a mild haploinsufficiency phenotype in cellular expression studies (<50% function loss), albeit with increased conductance, and the p.R518X (C-terminal) variant a nonsense mutation with a well-documented haploinsufficiency phenotype (50% function loss) (28). The compound heterozygous phenotype (p.S349W/p.R518X) is expected to result in a close to 90% *KCNQ1* function loss (19). In line with their pathogenic *KCNQ1* loss-of-function genotypes, both patients in our study have a QTc > 500 ms (indicating a high-risk clinical phenotype), a history of sympathetically triggered cardiac events, and share the triggers of short "burst" physical activities (running up the stairs, running for the bus, competing in team sports). Across all our electrophysiological data, the sympathetic neuronal hyperactivity phenotype is present in hiPSC-SNs from both patients. A potential genotype-phenotype correlation is apparent in the neuronal excitability and activity data, with significantly higher action potential frequency following current injection in sympathetic neurons from the compound heterozygous patient (p.S349W/p.R518X), compared with the heterozygous patient (c.781_782delinsTC). Moreover, p.S349W/p.R518X hiPSC-SNs present with significantly larger synaptic current amplitudes compared with c.781_782delinsTC hiPSC-

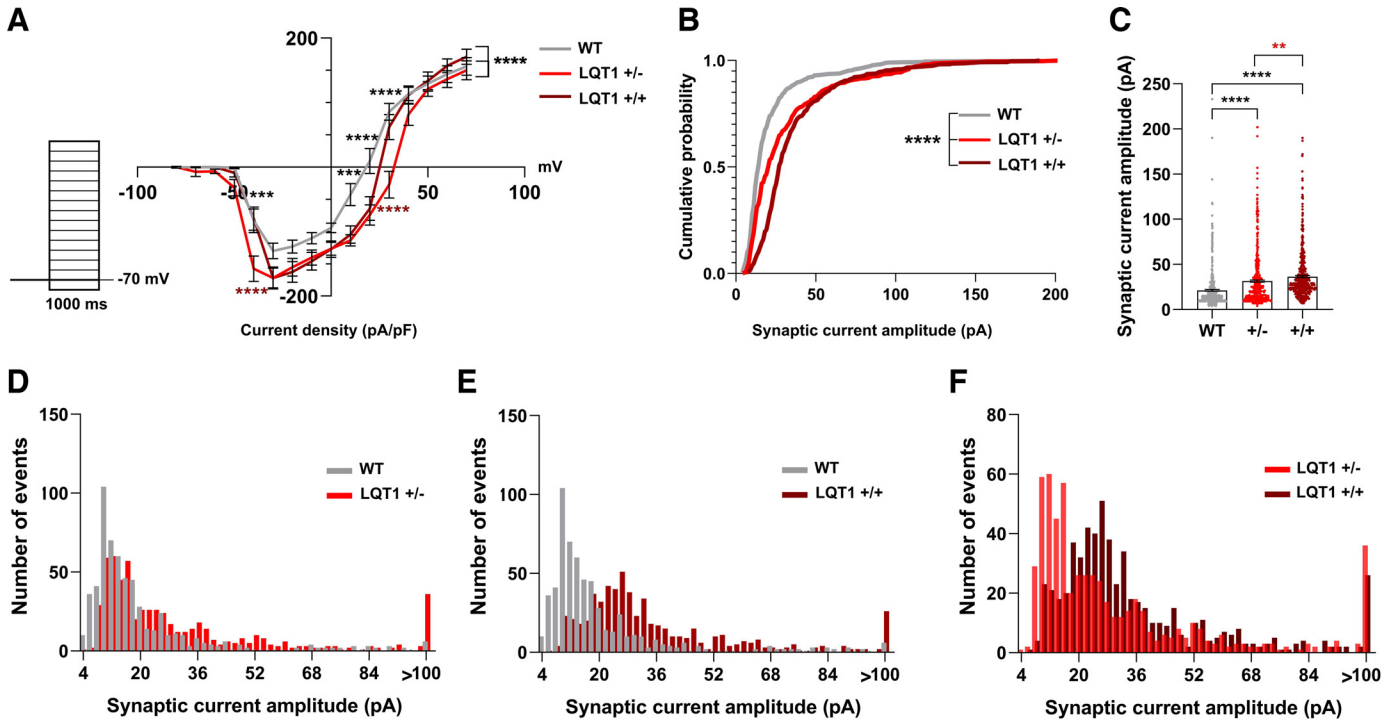

Figure 5. Total current density and synaptic current amplitudes in long QT syndrome type 1 (LQT1) human induced pluripotent stem cell (hiPSC)-derived sympathetic neurons of heterozygous (+/−) and compound heterozygous (+/+) *KCNQ1* genotype, compared with wild-type (WT) (−/−). *A*: total current density curves (with voltage protocol depicted to the left) revealed significant differences across LQT1 and WT genotypes ($P < 0.0001$, $n = 26$ c.781_782delinsTC; $n = 25$ p.S349W/p.R518X; $n = 23$ WT, analyzed by two-way ANOVA across the three groups). Specifically, total inward current densities were larger in LQT1 hiPSC-sympathetic neurons (hiPSC-SNs), with maximum current density between +10 mV and +30 mV (adjusted $P < 0.001$ to $P < 0.0001$, analyzed by ad hoc comparison using Tukey's multiple comparisons test, black asterisks). Significant differences between LQT1 (+/−) and LQT1 (+/+) genotypes were seen at −40 mV and +30 mV (adjusted $P < 0.0001$, red asterisks). Error bars represent standard error mean. *B–F*: synaptic current amplitudes recorded in voltage-clamp mode (−70 mV; 50 consecutive synaptic currents per cell), were significantly larger in LQT1 hiPSC-SNs ($P < 0.0001$, $n = 12$ c.781_782delinsTC; $n = 12$ p.S349W/p.R518X; $n = 12$ WT hiPSC-SNs, analyzed by one-way ANOVA across the three groups). *B*: cumulative probability plot. *C*: ad hoc subgroup analysis using Tukey's multiple comparisons test showed that both heterozygous LQT1 (+/−) and compound heterozygous LQT1 (+/+) hiPSC-SNs registered larger synaptic current amplitudes than WT hiPSC-SNs ($P < 0.0001$), and that synaptic currents were significantly larger in LQT1 (+/+, dark red) hiPSC-SNs compared with LQT1 (+/−, bright red) hiPSC-SNs, $P = 0.0038$. Error bars represent standard error mean. Amplitude frequency histograms depicting the distribution of all measured synaptic current amplitudes, $n = 600$ per genotype, using 2 pA bins, synaptic currents ≥100 pA binned together, (*D*) LQT1 (+/−, bright red) vs. WT (−/−, gray); (*E*) LQT1 (+/+, dark red) vs. WT (−/−, gray); (*F*) LQT1 (+/−, bright red) vs. LQT1 (+/+, dark red). All characterization (*A–F*) was performed in hiPSC-SNs ≥48 days in vitro (17). $^{**}P < 0.01$, $^{***}P < 0.001$, and $^{****}P < 0.0001$.

SNs, as apparent from the difference in the level of the rightward shift in the cumulative probability and the amplitude frequency graphs. These data support that the compound heterozygous LQT1 genotype might induce a higher magnitude increase in sympathetic neuron current transfer, suggesting that specific genotypes may have stronger cellular neuronal phenotypes. Such a genotype-phenotype correlation, corresponding to level of *KCNQ1* function loss and resultant effects on cellular and tissue function, is consistent with previous findings in patients with LQT1 with regards to cardiac and extracardiac phenotype presentations (19–22, 29). With regards to LQT1 cardiac phenotype from fetal life onward, clinical findings including intrauterine bradycardia, QT interval prolongation, and arrhythmia propensity are consistently more severe in patients with more pronounced *KCNQ1* function loss (homozygous/compound heterozygous genotype vs. heterozygous genotype, and, heterozygous dominant mutations vs. heterozygous haploinsufficiency mutations) (19, 20, 29). In addition to being expressed in the heart and neuronal networks, *KCNQ1*-encoded Kv7.1 potassium channels are expressed in the inner ear hair cells that are the sensory receptors of both the auditory system and the vestibular system, as well as in the kidneys, lungs, placenta, intestine, and stomach (7, 10). Previous studies have shown that patients with LQT1 with homozygous or compound heterozygous *KCNQ1* loss-of-function genotype also have extracardiac manifestations, including sensorineural deafness and vestibular dysfunction (19, 21). The conundrum by which the same *KCNQ1* loss-of-function mutations can cause a cardiac phenotype in the majority of carriers and sensorineural deafness in a select few was addressed in a publication with the poetic name "I_{Ks} in Heart and Hearing, the Ear Can Do with Less than the Heart," demonstrating that only a >90% *KCNQ1* function loss led to total sensorineural hearing loss (30). Further genotype-phenotype extracardiac manifestations of *KCNQ1* function loss include clinical symptoms from the gastrointestinal tract secondary to hypochlorhydria, resultant elevated gastrin levels, and iron-deficiency anemia in patients with homozygous/compound heterozygous LQT1, but not in patients with heterozygous LQT1 (22, 31). Taking our functional cellular data and previously published clinical data into consideration (19–22, 29), the neuronal LQT1 hiPSC-SN phenotype resembles the cardiac LQT1 phenotype in the way that a single pathogenic *KCNQ1* mutation may be sufficient for the phenotype to manifest (and

that the neuronal phenotype may be aggravated by further *KCNQ1* function loss), as compared with the auditory and gastrointestinal phenotypes that only manifest in patients with near-complete *KCNQ1* function loss. Characterization of the neuronal phenotype in a range of *KCNQ1* genotypes is needed to confirm a genotype-phenotype correlation and whether neuronal hyperactivity is common in LQT1.

Focusing on the LQT1 neuronal phenotype, we observed that LQT1 hiPSC-SN cultures released higher levels of norepinephrine, in line with our findings that LQT1 hiPSC-SNs were more likely to fire spontaneous action potentials, and exhibited larger synaptic current amplitudes, compared with WT hiPSC-SNs. In our study, norepinephrine release was reduced or abolished following sodium channel block with 1 μM TTX, showing the source of norepinephrine release in these cells is largely in response to evoked Na^+-channel-dependent action potentials. Similar results were seen in an early study on mechanisms of norepinephrine release in the isolated rat kidney, where 0.3 μM TTX abolished the effect of nerve stimulation on norepinephrine release (32). Early studies on mechanisms of norepinephrine release in rat sympathetic neurons have shown that increased ganglionic transmission via activation of nicotinic receptors increases the activity of tyrosine hydroxylase, the enzyme that catalyzes the rate-limiting step in catecholamine biosynthesis (33). The increase in enzyme activity is of two types, an acute increase and a delayed and long-lasting increase, supporting that periods of increased synaptic stimulation can alter the protein composition of sympathetic neurons, increasing tyrosine hydroxylase activity and thus norepinephrine biosynthesis (33). The increase in norepinephrine release observed in our neurons from patients with LQT1 could therefore cause a consequent increase in tyrosine hydroxylase to result in a perpetuating increase in noradrenergic synaptic transmission in LQT1. Further studies are needed to elucidate the mechanisms of changes in synaptic strength occurring in LQT1 SNs, including examination of SNs forming synaptic connections not only with CMs but also with other SNs in vivo, as occurs in our hiPSC-SNs in vitro (17), providing a mechanism for titrating neuronal output to the heart.

Increased release of norepinephrine has been reported in several disease states associated with sympathetic dysautonomia, where increased neurotransmitter release regulates further presynaptic transmitter release via a positive feedback pathway (1, 2, 34). Norepinephrine increases calcium ion influx and secondary calcium release via L-type calcium channels in cardiomyocytes and N-type calcium channels in neurons (1, 2, 34). This norepinephrine-related increase in calcium influx is consistent with our finding of an increased total inward current between +10 mV to +30 mV in LQT1 hiPSC-SNs of both heterozygous and compound heterozygous genotypes (1, 2, 34). In the setting of LQT1, increased norepinephrine secretion and resultant increased calcium influx in neurons and cardiomyocytes would further aggravate the pre-existing arrhythmia propensity (1, 2, 24, 34–36).

The mechanisms underpinning how Kv7.1-related alterations in sympathetic neuron excitability could contribute to LQT1 is of significant interest. We know from previous studies that loss-of-function in Kv7.2 and Kv7.3 subunits are both associated with neuronal hyperactivity and epilepsy (37). Kv7.2 and Kv7.3 subunits underlie the neuronal M-current (I_{KM}), and inhibition of these channels facilitates repetitive discharges and conversion from phasic to tonic firing pattern in sympathetic neurons (37). Blocking I_{KM} with XE991 in rat sympathetic neurons reduces the outward current, suppresses the slow deactivation relaxation, and promotes repetitive spike discharges by a relative lowering of the threshold for subsequent spikes (37). The resultant increased spike frequency increases calcium influx via N-type calcium channels and further increases spike frequency, via the mechanisms discussed (1, 2, 34, 37). In our electrophysiological data, the finding that all LQT1 hiPSC-SNs presented with a tonic firing pattern, including a higher frequency of spike discharges compared with WT tonic hiPSC-SNs, in conjunction with the increased levels of norepinephrine secretion and increased total inward current between +10 mV to +30 mV, suggests a similar mechanism could underlie the findings in human-derived sympathetic neurons with Kv7.1 loss-of-function. Indeed, one hypothesis relates to the observed changes in LQT1 hiPSC-SN afterhyperpolarization kinetics. A sympathetic neuronal action potential is normally followed by an inactivating AHP with a short to medium duration of up to 428 ms (1, 15, 17, 34, 37). However, we noted a significant lack of AHP in 57% of LQT1 hiPSC-SNs, and a propensity for excitatory postsynaptic potentials and triggered activity following LQT1 spontaneous spike discharges, suggesting that failed neuronal inactivation via hyperpolarization might contribute to the increased LQT1 hiPSC-SNs activity. As such, decreased outward current, decreased threshold for subsequent spike discharge, and resultant neuronal hyperactivity could potentially represent a mechanistic link between *KCNQ1* loss-of-function and neuronal hyperactivity in LQT1 hiPSC-SNs.

Although this is the first report of an electrophysiological disease phenotype in LQTS sympathetic neurons, low-grade inflammation of the stellate ganglia of patients with LQTS has been previously described in postmortem findings and stellectomy specimens, albeit of unclear significance (38–40). There is moreover a strong neurocardiac connection in LQTS with regards to the neuronal nitric oxide synthase adaptive protein NOS1AP (2). NOS1AP is expressed in both sympathetic neurons and ventricular cardiomyocytes, and *NOS1AP* loss-of-function variants are associated with both sympathetic neuronal hyperactivity, driven by increased activity in N-type calcium channels, and loss of inhibition of L-type calcium channels in ventricular cardiomyocytes, leading to reduced repolarization and increased arrhythmia propensity (2, 34). This illustrates how sympathetic hyperactivity and compromised cardiac repolarization can be intrinsically linked in inducing LQTS arrhythmia (2). Therefore, in addition to the cellular effects of *KCNQ1*-associated LQT1 mutations on cardiomyocyte repolarization previously described (12–14), our data identify an additional neuronal phenotype for LQT1 suggesting that these phenotypes in the two cell types compound in sympathetically triggered LQT1 arrhythmia. Our data also highlight that identifying sympathetic neuronal contributions to LQT1 and other sympathetic cardiovascular disorders requires the examination of both sympathetic neurons and neuro-cardiomyocyte interactions (41), rather than assessing responses to sympathomimetics in cardiomyocyte monoculture.

Conclusions

We have established human LQT1 norepinephrine-secreting and electrophysiologically functional hiPSC-derived sympathetic neurons. By studying LQT1 hiPSC-derived sympathetic neurons in monoculture we have identified a novel LQT1 phenotype of increased neurotransmission and neuronal hyperactivity that could contribute to the mechanisms underlying sympathetically triggered arrhythmia.

ACKNOWLEDGMENTS

We acknowledge the participating patients and whanau (extended families).

Present address of J. R. Skinner: Cardiac Services, Heart Centre for Children, Sydney Children's Hospital Network, Sydney, Australia.

GRANTS

A. Winbo was funded by the Heart Foundation New Zealand, the Hugh Green Foundation, Cure Kids, the Auckland Medical Research Foundation, SJ Taylor Fund, School of Medicine Foundation, the Swedish Research Council, and the Swedish Heart and Lung Foundation.

DISCLAIMERS

Data were collected with the ethics requirement that patients' data are confidential and will not be shared. Any questions should be directed to the corresponding author.

DISCLOSURES

No conflicts of interest, financial or otherwise, are declared by the authors.

AUTHOR CONTRIBUTIONS

A.W., A.R., S.J., J.R.S., and J.M.M. conceived and designed research; A.W. and S.R. performed experiments; A.W. analyzed data; A.W. and J.M.M. interpreted results of experiments; A.W. prepared figures; A.W. drafted manuscript; A.W., A.R., S.J., J.R.S., and J.M.M. edited and revised manuscript; A.W., S.R., E.E., A.R., S.J., J.R.S., and J.M.M. approved final version of manuscript.

REFERENCES

1. **Herring N**, **Kalla M**, **Paterson DJ.** The autonomic nervous system and cardiac arrhythmias: current concepts and emerging therapies. *Nat Rev Cardiol* 16: 707–726, 2019 [Erratum in *Nat Rev Cardiol* 16:760, 2019]. doi:10.1038/s41569-019-0221-2.
2. **Winbo A**, **Paterson DJ.** The brain-heart connection in sympathetically triggered inherited arrhythmia syndromes. *Heart Lung Circ* 29: 529–537, 2020. doi:10.1016/j.hlc.2019.11.002.
3. **Ackerman MJ**, **Khositseth A**, **Tester DJ**, **Hejlik JB**, **Shen WK**, **Porter CB.** Epinephrine-induced QT interval prolongation: a gene-specific paradoxical response in congenital long QT syndrome. *Mayo Clin Proc* 77: 413–421, 2002. doi:10.4065/77.5.413.
4. **Schwartz PJ.** Another role for the sympathetic nervous system in the long QT syndrome? *J Cardiovasc Electrophysiol* 12: 500–502, 2001. doi:10.1046/j.1540-8167.2001.00500.x.
5. **Skinner JR**, **Winbo A**, **Abrams D**, **Vohra J**, **Wilde AA.** Channelopathies that lead to sudden cardiac death: clinical and genetic aspects. *Heart Lung Circ* 28: 22–30, 2019. doi:10.1016/j.hlc.2018.09.007.
6. **Barhanin J**, **Lesage F**, **Guillemare E**, **Fink M**, **Lazdunski M**, **Romey G.** K_VLQT1 and IsK (minK) proteins associate to form the I_{KS} cardiac potassium current. *Nature* 384: 78–80, 1996. doi:10.1038/384078a0.
7. **Jespersen T**, **Grunnet M**, **Olesen SP.** The KCNQ1 potassium channel: from gene to physiological function. *Physiology (Bethesda, MD)* 20: 408–416, 2005. doi:10.1152/physiol.00031.2005.
8. **Sanguinetti MC**, **Curran ME**, **Zou A**, **Shen J**, **Spector PS**, **Atkinson DL**, **Keating MT.** Coassembly of K(V)LQT1 and minK (IsK) proteins to form cardiac I(Ks) potassium channel. *Nature* 384: 80–83, 1996. doi:10.1038/384080a0.
9. **Shimizu W**, **Antzelevitch C.** Cellular basis for the ECG features of the LQT1 form of the long-QT syndrome: effects of beta-adrenergic agonists and antagonists and sodium channel blockers on transmural dispersion of repolarization and torsade de pointes. *Circulation* 98: 2314–2322, 1998. doi:10.1161/01.cir.98.21.2314.
10. **Goldman AM**, **Glasscock E**, **Yoo J**, **Chen TT**, **Klassen TL**, **Noebels JL.** Arrhythmia in heart and brain: KCNQ1 mutations link epilepsy and sudden unexplained death. *Sci Transl Med* 1: 2ra6, 2009. doi:10.1126/scitranslmed.3000289.
11. **Johnson JN**, **Hofman N**, **Haglund CM**, **Cascino GD**, **Wilde AA**, **Ackerman MJ.** Identification of a possible pathogenic link between congenital long QT syndrome and epilepsy. *Neurology* 72: 224–231, 2009. doi:10.1212/01.wnl.0000335760.02995.ca.
12. **Egashira T**, **Yuasa S**, **Suzuki T**, **Aizawa Y**, **Yamakawa H**, **Matsuhashi T**, **Ohno Y**, **Tohyama S**, **Okata S**, **Seki T**, **Kuroda Y**, **Yae K**, **Hashimoto H**, **Tanaka T**, **Hattori F**, **Sato T**, **Miyoshi S**, **Takatsuki S**, **Murata M**, **Kurokawa J**, **Furukawa T**, **Makita N**, **Aiba T**, **Shimizu W**, **Horie M**, **Kamiya K**, **Kodama I**, **Ogawa S**, **Fukuda K.** Disease characterization using LQTS-specific induced pluripotent stem cells. *Cardiovasc Res* 95: 419–429, 2012. doi:10.1093/cvr/cvs206.
13. **Itzhaki I**, **Maizels L**, **Huber I**, **Zwi-Dantsis L**, **Caspi O**, **Winterstern A**, **Feldman O**, **Gepstein A**, **Arbel G**, **Hammerman H**, **Boulos M**, **Gepstein L.** Modelling the long QT syndrome with induced pluripotent stem cells. *Nature* 471: 225–229, 2011. doi:10.1038/nature09747.
14. **Moretti A**, **Bellin M**, **Welling A**, **Jung CB**, **Lam JT**, **Bott-Flugel L**, **Dorn T**, **Goedel A**, **Hohnke C**, **Hofmann F**, **Seyfarth M**, **Sinnecker D**, **Schomig A**, **Laugwitz KL.** Patient-specific induced pluripotent stem-cell models for long-QT syndrome. *N Engl J Med* 363: 1397–1409, 2010. doi:10.1056/NEJMoa0908679.
15. **Oh Y**, **Cho GS**, **Li Z**, **Hong I**, **Zhu R**, **Kim MJ**, **Kim YJ**, **Tampakakis E**, **Tung L**, **Huganir R**, **Dong X**, **Kwon C**, **Lee G.** Functional coupling with cardiac muscle promotes maturation of hPSC-derived sympathetic neurons. *Cell stem cell* 19: 95–106, 2016. doi:10.1016/j.stem.2016.05.002.
16. **Takayama Y**, **Kushige H**, **Akagi Y**, **Suzuki Y**, **Kumagai Y**, **Kida YS.** Selective induction of human autonomic neurons enables precise control of cardiomyocyte beating. *Sci Rep* 10: 9464, 2020. doi:10.1038/s41598-020-66303-3.
17. **Winbo A**, **Ramanan S**, **Eugster E**, **Jovinge S**, **Skinner JR**, **Montgomery JM.** Functional coculture of sympathetic neurons and cardiomyocytes derived from human-induced pluripotent stem cells. *Am J Physiol Heart Circ Physiol* 319: H927–H937, 2020. doi:10.1152/ajpheart.00546.2020.
18. **Leong IUS**, **Dryland PA**, **Prosser DO**, **Lai SW**, **Graham M**, **Stiles M**, **Crawford J**, **Skinner JR**, **Love DR.** Splice site variants in the KCNQ1 and SCN5A genes: transcript analysis as a tool in supporting pathogenicity. *J Clin Med Res* 9: 709–718, 2017. doi:10.14740/jocmr2894w.
19. **Winbo A**, **Stattin EL**, **Diamant UB**, **Persson J**, **Jensen SM**, **Rydberg A.** Prevalence, mutation spectrum, and cardiac phenotype of the Jervell and Lange-Nielsen syndrome in Sweden. *Europace* 14: 1799–1806, 2012. doi:10.1093/europace/eus111.
20. **Winbo A**, **Fosdal I**, **Lindh M**, **Diamant UB**, **Persson J**, **Wettrell G**, **Rydberg A.** Third trimester fetal heart rate predicts phenotype and mutation burden in the type 1 long QT syndrome. *Circ Arrhythm Electrophysiol* 8: 806–814, 2015. doi:10.1161/CIRCEP.114.002552.
21. **Winbo A**, **Rydberg A.** Vestibular dysfunction is a clinical feature of the Jervell and Lange-Nielsen Syndrome. *Scand Cardiovasc J* 49: 7–13, 2015. doi:10.3109/14017431.2014.988172.
22. **Winbo A**, **Sandstrom O**, **Palmqvist R**, **Rydberg A.** Iron-deficiency anaemia, gastric hyperplasia, and elevated gastrin levels due to potassium channel dysfunction in the Jervell and Lange-Nielsen Syndrome. *Cardiol Young* 23: 325–334, 2013. doi:10.1017/S1047951112001060.
23. **Chambers SM**, **Mica Y**, **Studer L**, **Tomishima MJ.** Converting human pluripotent stem cells to neural tissue and neurons to model

neurodegeneration. *Methods Mol Biol (Clifton, NJ)* 793: 87–97, 2011. doi:10.1007/978-1-61779-328-8_6.

24. **Marban E**, **Robinson SW**, **Wier WG.** Mechanisms of arrhythmogenic delayed and early afterdepolarizations in ferret ventricular muscle. *J Clin Invest* 78: 1185–1192, 1986. doi:10.1172/JCI112701.
25. **McKeon A**, **Vaughan C**, **Delanty N.** Seizure versus syncope. *Lancet Neurol* 5: 171–180, 2006 [Erratum in *Lancet Neurol* 5: 293, 2006]. doi:10.1016/S1474-4422(06)70350-7.
26. **Opherk C**, **Coromilas J**, **Hirsch LJ.** Heart rate and EKG changes in 102 seizures: analysis of influencing factors. *Epilepsy Res* 52: 117–127, 2002. doi:10.1016/s0920-1211(02)00215-2.
27. **Zijlmans M**, **Flanagan D**, **Gotman J.** Heart rate changes and ECG abnormalities during epileptic seizures: prevalence and definition of an objective clinical sign. *Epilepsia* 43: 847–854, 2002. doi:10.1046/j.1528-1157.2002.37801.x.
28. **Horr S**, **Goldenberg I**, **Moss AJ**, **J OU**, **Barsheshet A**, **Connelly H**, **Gray DA**, **Zareba W**, **Lopes CM.** Ion channel mechanisms related to sudden cardiac death in phenotype-negative long-QT syndrome genotype-phenotype correlations of the KCNQ1(S349W) mutation. *J Cardiovasc Electrophysiol* 22: no–200, 2010. doi:10.1111/j.1540-8167.2010.01852.x.
29. **Winbo A**, **Rydberg A.** Fetal heart rate reflects mutation burden and clinical outcome in twin probands with KCNQ1 mutations. *HeartRhythm case Rep* 4: 237–240, 2018. doi:10.1016/j.hrcr.2018.02.008.
30. **Bhuiyan ZA**, **Wilde AA.** IKs in heart and hearing, the ear can do with less than the heart. *Circ Cardiovasc Genet* 6: 141–143, 2013. doi:10.1161/CIRCGENETICS.113.000143.
31. **Rice KS**, **Dickson G**, **Lane M**, **Crawford J**, **Chung SK**, **Rees MI**, **Shelling AN**, **Love DR**, **Skinner JR.** Elevated serum gastrin levels in Jervell and Lange-Nielsen syndrome: a marker of severe KCNQ1 dysfunction? *Heart Rhythm* 8: 551–554, 2011. doi:10.1016/j.hrthm.2010.11.039.
32. **el-Din MM**, **Malik KU.** Mechanism of norepinephrine release elicited by renal nerve stimulation, veratridine and potassium chloride in the isolated rat kidney. *J Pharmacol Exp Ther* 243: 76–85, 1987.
33. **Zigmond RE.** A comparison of the long-term and short-term regulations of tyrosine hydroxylase activity. *J Physiol (Paris)* 83: 267–271, 1988.
34. **Bardsley EN**, **Davis H**, **Buckler KJ**, **Paterson DJ.** Neurotransmitter switching coupled to β-adrenergic signaling in sympathetic neurons in prehypertensive states. *Hypertension* 71: 1226–1238, 2018. doi:10.1161/HYPERTENSIONAHA.118.10844.
35. **Shen MJ**, **Zipes DP.** Role of the autonomic nervous system in modulating cardiac arrhythmias. *Circ Res* 114: 1004–1021, 2014. doi:10.1161/CIRCRESAHA.113.302549.
36. **Yue DT**, **Herzig S**, **Marban E.** Beta-adrenergic stimulation of calcium channels occurs by potentiation of high-activity gating modes. *Proc Natl Acad Sci USA* 87: 753–757, 1990. doi:10.1073/pnas.87.2.753.
37. **Brown DA**, **Passmore GM.** Neural KCNQ (Kv7) channels. *Br J Pharmacol* 156: 1185–1195, 2009. doi:10.1111/j.1476-5381.2009.00111.x.
38. **James TN**, **Froggatt P**, **Atkinson WJ Jr**, **Lurie PR**, **McNamara DG**, **Miller WW**, **Schloss GT**, **Carroll JF**, **North RL.** De subitaneis mortibus. XXX. Observations on the pathophysiology of the long QT syndromes with special reference to the neuropathology of the heart. *Circulation* 57: 1221–1231, 1978. doi:10.1161/01.cir.57.6.1221.
39. **Pfeiffer D**, **Fiehring H**, **Henkel HG**, **Rostock KJ**, **Rathgen K.** Long QT syndrome associated with inflammatory degeneration of the stellate ganglia. *Clin Cardiol* 12: 222–224, 1989. doi:10.1002/clc.4960120408.
40. **Rizzo S**, **Basso C**, **Troost D**, **Aronica E**, **Frigo AC**, **Driessen AH**, **Thiene G**, **Wilde AA**, **van der Wal AC.** T-cell-mediated inflammatory activity in the stellate ganglia of patients with ion-channel disease and severe ventricular arrhythmias. *Circ Arrhythm Electrophysiol* 7: 224–229, 2014. doi:10.1161/CIRCEP.113.001184.
41. **Larsen HE**, **Lefkimmiatis K**, **Paterson DJ.** Sympathetic neurons are a powerful driver of myocyte function in cardiovascular disease. *Sci Rep* 6: 38898, 2016. doi:10.1038/srep38898.